ChemPubSoc Europe

DOI: 10.1002/cssc.201403345

CHEMSUSCHEM Communications

Photocatalytic Carbon Dioxide Reduction with Rhodium-based Catalysts in Solution and Heterogenized within Metal–Organic Frameworks

Matthew B. Chambers,[a] Xia Wang,[a] Noémie Elgrishi,[a] Christopher H. Hendon,[d] Aron Walsh,[d] Jonathan Bonnefoy,[c] Jérôme Canivet,[c] Elsje Alessandra Quadrelli,[b] David Farrusseng,[c] Caroline Mellot-Draznieks,[a] and Marc Fontecave*[a]

The first photosensitization of a rhodium-based catalytic system for CO_2 reduction is reported, with formate as the sole carbon-containing product. Formate has wide industrial applications and is seen as valuable within fuel cell technologies as well as an interesting H_2-storage compound. Heterogenization of molecular rhodium catalysts is accomplished via the synthesis, post-synthetic linker exchange, and characterization of a new metal–organic framework (MOF) Cp*Rh@UiO-67. While the catalytic activities of the homogeneous and heterogeneous systems are found to be comparable, the MOF-based system is more stable and selective. Furthermore it can be recycled without loss of activity. For formate production, an optimal catalyst loading of ~10% molar Rh incorporation is determined. Increased incorporation of rhodium catalyst favors thermal decomposition of formate into H_2. There is no precedent for a MOF catalyzing the latter reaction so far.

Practical reduction of carbon dioxide (CO_2) requires mediating multielectron and multiproton processes while achieving desired product selectivity in a cost-effective manner. Discrete molecular catalysts have been shown to be invaluable in achieving CO_2 reduction while maintaining synthetic control over the selectivity of the products within homogeneous systems.[1] However, homogeneous catalysis often suffers from additional costs associated with use of solvents, product isolation, and catalyst recovery, amongst other factors.[2] Heterogeneous catalysis has the potential to avoid such expenses but often fails to achieve easily tunable optimization and product selectivity, which is a crucial aspect of CO_2-reduction chemistry.[3] Therefore, the integration of molecular catalysts into solid-state systems offers the possibility to maintain the advantageous properties of homogeneous catalysis while moving towards practical system designs afforded by heterogeneous catalysis.

Among heterogenization methodologies, the incorporation of active molecular catalysts into the framework of hybrid materials gives access to advantageous catalytic solids.[4] The crystalline nature of metal–organic frameworks (MOFs) makes this class of porous solids promising as model materials for the grafting of single-site catalytic organometallics, especially through post-synthetic modifications.[5] Unlike the situation for homogeneous catalysis, the covalent grafting of single-site organometallic species within high-surface-area supports can essentially eliminate the involvement of unexpected dimeric species, which might lead to catalyst deactivation[6] or undesired reactions,[7] by site isolation of the catalytic species.[8] This has usually been achieved by using ordered porous silicas, such as MCM or SBA solids.[9] The monomeric nature of grafted molecular complexes within MOFs is rarely characterized by direct means.[5b,i,10] Surprisingly, very few examples of the incorporation of CO_2 reduction homogeneous catalysts into MOFs for CO_2 photoreduction have been reported so far.[11] Previous reports appear limited to a rhenium–carbonyl photocatalyst included into a MOF for selective CO production[11a] and an iridium-based system within a nonporous coordination polymer for formate production.[11b] Within these examples, the immobilized organometallic species serves as both the light-absorbing entity and as the CO_2-reduction catalyst. However, given the potential of highly tuneable and optimized MOFs,[12] our strategy consists in decoupling and independently optimizing the light absorption and catalytic functions within these hybrid materials. To our knowledge, this strategy has never been achieved for CO_2 reduction.

Herein, we report our initial efforts (i) to identify a novel selective molecular photocatalytic system for the reduction of CO_2 into formate, and (ii) to incorporate the catalyst into a MOF as part of the framework while evaluating performance parameters regarding activity, stability, and product selectivity during CO_2 photoreduction using a soluble photosensitizer, $[Ru(bpy)_3]Cl_2$ (bpy = 2,2′-bipyridine).

The catalyst scope of our study has been limited to the "Cp*Rh" (Cp* = pentamethylcyclopentadiene) class of complexes. Cp*Rh-based complexes have been widely reported for

[a] Dr. M. B. Chambers, X. Wang, N. Elgrishi, Dr. C. Mellot-Draznieks, Prof. M. Fontecave
Laboratoire de Chimie des Processus Biologiques, UMR 8229 CNRS, UPMC Univ Paris 06, Collège de France, 11 Marcelin Berthelot, 75231 Paris Cedex 05, France
Fax: +33 1 44271356 ; Tel: +33 1 44271360
E-mail: marc.fontecave@cea.fr

[b] Dr. E. A. Quadrelli
IRCELYON, Université Lyon 1 - CNRS, UMR 5256
2, av. Albert Einstein, 69626 Villeurbanne (France)

[c] J. Bonnefoy, Dr. J. Canivet, Dr. D. Farrusseng
C2P2, Université Lyon 1 - CPE - CNRS, UMR 5265
43, bdv du 11 Novembre 1918, 69616 Villeurbanne (France)

[d] Dr. C. H. Hendon, Dr. A. Walsh
Department of Chemistry, University of Bath
Claverton, Bath BA2 7AY (UK)

Supporting Information for this article is available on the WWW under http://dx.doi.org/10.1002/cssc.201403345.

the catalytic reduction of NAD^+ enzyme cofactor.[13] Deronzier and co-workers have previously reported $Cp^*Rh(bpy)Cl_2$ to electrocatalytically reduce CO_2 to a mixture of formate and hydrogen.[14] Recently, formate production from CO_2 has garnered widespread interest due the intrinsic value of formate within fuel-cell technologies, as a means to store H_2 and various other industrial applications.[15] Of note, operative mechanisms within formic acid fuel cells commonly invoke preliminary deprotonation of formic acid to generate formate prior to energy conversion processes.[16]

The molecular compounds evaluated within this work are $Cp^*Rh(bpy)Cl_2$ (**1**) and $Cp^*Rh(bpydc)Cl_2$ (bpydc = 2,2′-bipyridine-5,5′-dicarboxylic acid) (**2**), having in mind that **2** can act as linker in MOFs. As the Cp*Rh class of compounds has solely been evaluated electrochemically as a CO_2 reduction catalyst, this work represents the first successful study in which rhodium-based compounds are integrated into photochemical systems of any kind for CO_2 reduction. Compounds **1** and **2** were synthesized utilizing previously reported methods.[17] A crystal structure of **2** is presented in the Supporting Information (Figure S1) and shows the typical stool-like coordination geometry for these complexes. The catalytic performances of molecular complexes **1** and **2** are also compared to those of rhodium-functionalized MOF solids, as detailed below.

We have selected the MOF UiO-67,[18] formulated as $Zr_6(OH)_4(O)_4(O_2C\text{-}C_6H_4\text{-}C_6H_4\text{-}CO_2)_6$, as immobilization platform for the Cp*Rh catalyst. Its large pore size and general stability to water, ambient air, and high temperatures make UiO-67 suitable for post-synthetic modifications. Following post-synthetic ligand exchange methodology,[5i] we reacted UiO-67 with the synthesized molecular complex **2** in deionized water at room temperature for 24 h (Scheme 1). The variation of the amount

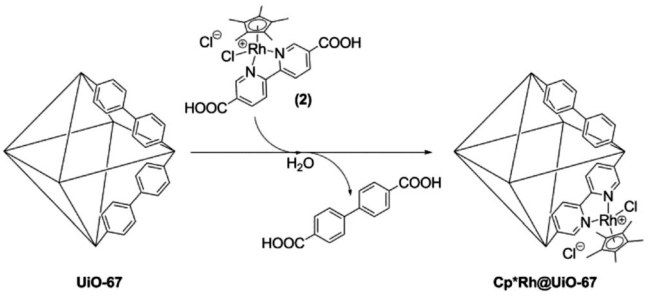

Scheme 1. Heterogenization of a rhodium complex into the framework of UiO-67 through post-synthetic linker exchange.

of **2** in the post-synthetic exchange yielded a series of four rhodium-functionalized MOFs, namely 5%-, 10%-, 20%-, and 35%-Cp*Rh@UiO-67, isoreticular to their parent UiO-67 in which respectively 5, 10, 20, and 35% of the parent 4,4′-biphenyldicarboxylate (bpdc) linkers are exchanged with **2**. The percentages of linker exchange were determined by liquid ^1H NMR analysis of dissolved samples of Cp*Rh@UiO-67 by comparison of the signals integrations of the biphenyl and bipyridine linkers (Supporting Information, Figure S4). Elemental analysis confirmed that the weight-percent ratios of Zr:Rh for all prepared samples are in line with the theoretical values calculated from percentages of linker exchange found by NMR (Supporting Information, Table S2). Scanning electron microscopy (SEM) was performed on the MOFs and the images demonstrated constant particle shape and size (ca. 1 μm) across the samples (Supporting Information, pp. S17).

The following results, based on current state-of-the-art protocols,[5] are consistent with incorporation of complex **2** into the UiO-67 framework to give the Cp*Rh@UiO-67 solid. As the most direct evidence for the reaction shown in Scheme 1, during synthesis of the 10%-Cp*Rh@UiO-67 sample, the linker exchange reaction was performed in D_2O and the release of bpdc in solution was determined by ^1H NMR analysis of the supernatant. In perfect agreement with the stoichiometry of the reaction reported in Scheme 1, 10 mol% of bpdc was recovered in solution after the reaction. Furthermore, repeated washings with H_2O did not result in detectable liberation of **2**. When the same procedure was applied to complex **1**, uptake of **1** by UiO-67 was observed however with no parallel release of bpdc in solution. In that case **1** could be recovered by washing with H_2O (see Supporting Information, pp. S14–S16 for details).

The data shown in Figure 1 provide further support for the direct incorporation of **2** within the MOF scaffold. Brunauer–Emmett–Teller (BET) surface area measurements (Figure 1a and Supporting Information, Table S1) estimated from the nitrogen adsorption isotherms for the four Cp*Rh@UiO-67 samples show expected correlation between decreased surfaces area and increased rhodium incorporation. Furthermore, as expected, porosity values are also found to decrease gradually with increased rhodium incorporation (Figure 1a). The powder X-ray diffraction patterns before and after post-synthetic exchange confirmed the retention of the crystalline UiO-67 framework, with however a partial loss of crystallinity for the 35%-Cp*Rh@UiO-67 (Figure 1c) (For details, see Supporting Information, pp. S4–S7). Finally, diffuse reflectance spectra of 5%-, 10%-, 20%-, and 35%-Cp*Rh@UiO-67 (Figure 1b) allowed determination of an optical band gap (BG) value of 2.4 eV, independent of % rhodium incorporation. The intensity of the low-energy feature was found to increase as a function of rhodium incorporation. The optical BG value, which represents a decrease of 1.2 eV relative to the parent UiO-67,[19] is in perfect agreement with that computed via state-of-the-art electronic structure DFT calculations on a model of Cp*Rh@UiO-67 (Supporting Information, Figure S6). These calculations assign the BG to a rhodium-localized d–d transition, in agreement with the intensity variations observed in spectra in Figure 1b.

Photochemical assays were performed in a 1 cm quartz cuvette maintained at 20 °C using a mixture of acetonitrile and triethanolamine (TEOA) (5:1 volumetric ratio) as the solvent, with TEOA as both an electron and proton donor, in the presence of 1.0 mM $Ru(bpy)_3Cl_2$ as the photosensitizer. $Ru(bpy)_3Cl_2$ has recently been shown to effectively diffuse into the pores of UiO-67.[20] Compounds **1** and **2** were evaluated for activity at concentrations of 0.1 mM (0.08 μmol of Rh). Assays on MOF-based catalysts were performed using 1.4 mg of solid (corresponding to 0.04, 0.09, 0.16, and 0.28 μmol of rhodium in the

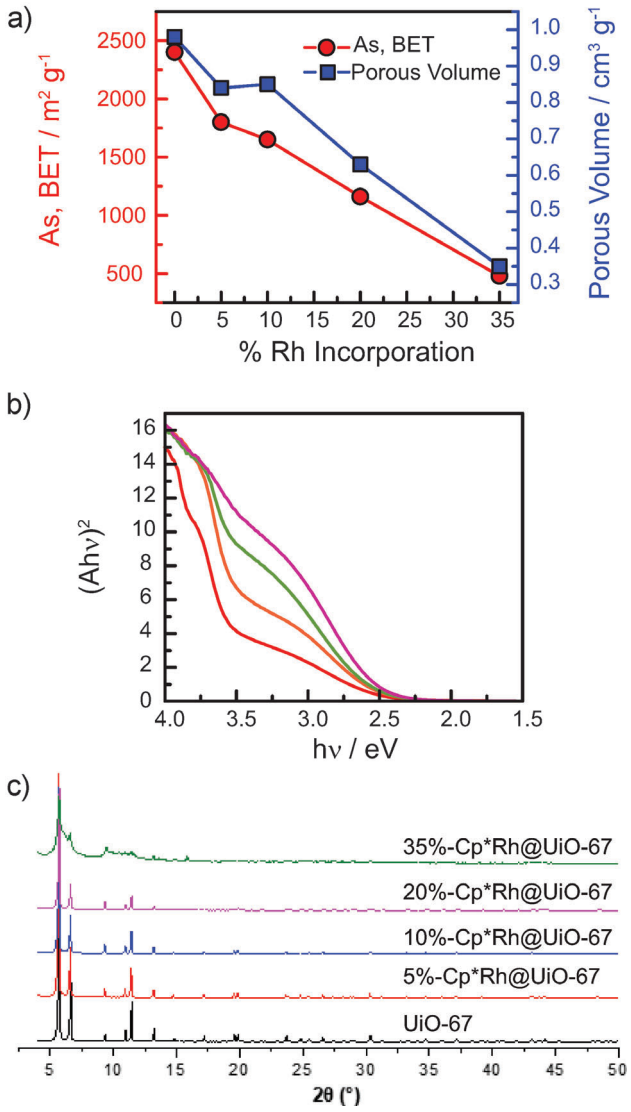

Figure 1. a) Surface area (red) and porosity (blue) values of Cp*Rh@UiO-67 as a function of % molar incorporation of **2**. b) Transformed diffuse reflectance spectra of Cp*Rh@UiO-67 with 5% (red), 10% (orange), 20% (green) and 35% (purple) molar incorporation of **2**. c) PXRD patterns for UiO-67 and Cp*Rh@UiO-67 samples with various molar incorporation of **2**.

5%, 10%, 20% and 35% loading, respectively). CO_2-saturated samples were irradiated by a 300 W Xe arc lamp equipped with a 415 nm cutoff filter and were vigorously stirred during the photolysis. As control experiments we found that both UiO-67 MOF and bpydc substituted analogues were inactive in the absence of the photosensitizer. Note that the large computed BG value of 3.6 eV for UiO-67 and UiO-67-bpydc models are representative of wide band gap insulators and make absorption of visible light by these compounds impossible (Supporting Information, Figure S6). Furthermore UiO-67 MOF was also inactive in the presence of the photosensitizer (Supporting Information, pp. S10).[21]

Both complexes **1** and **2** showed good activity during selective CO_2 photoreduction into formate (TON = 125 and 42 for **1** and **2** respectively after 10 h reaction) as the only carbon-containing product detected in appreciable quantities (no detection of carbon monoxide, methane, methanol, formaldehyde, oxalate, or ethylene). H_2 was the only other product of the reaction (TON = 55 and 38 for **1** and **2** respectively after 10 h reaction). Interestingly, these performances are comparable to those reported for the best homogeneous systems based on rhenium and ruthenium catalysts and $[Ru(bpy)_3]Cl_2$.[22] Furthermore, the photocatalytic selectivity of compounds **1** and **2** appears to be in the same range as that which Deronzier and co-workers have reported for the electrocatalytic systems: TONs between 16 and 25 for formate electroproduction and TONs between 6 and 14 for concomitant H_2 production for 1 to 3 h electrolyses.[14] This suggests that light absorption does not necessarily disrupts the reaction intermediates, unlike in recent manganese-based systems where products distribution drastically changes upon shifting a CO_2 reduction electrocatalyst into a photochemical system.[23]

The ca. 66% decrease in formate production between catalysts **1** and **2** agrees with a previously reported generalized trend wherein electron-rich ancillary ligands afford higher rates for CO_2 reduction.[24] This is further exemplified in the turnover frequency (TOF) at early time points for formate production of 20 h^{-1} and 10 h^{-1} for **1** and **2** respectively (Supporting Information, Figures S7 and S8).The molecular complex **2** represents the more appropriate comparison to the activity of Cp*Rh@UiO-67, as the carboxylic acid functionality is required for incorporation within the MOF and **2** is directly used for the post-synthetic exchange.

Photolysis of 1.4 mg of 10%-Cp*Rh@UiO-67 (10% molar incorporation of Cp*Rh approximately corresponding to 0.09 μmol Rh) during 10 h gave TON values comparable to those obtained during photolysis of **2** (0.08 μmol of Rh for 0.8 mL of 0.1 mM solutions of **2**): TON[formate] = 47 vs 42 and TON[H_2] = 36 vs 38 for solid MOF vs molecular **2**. The kinetic evolutions of formate generated by 10%-Cp*Rh@UiO-67 and **2** are shown in Figure 2 and indeed indicate comparable rates as

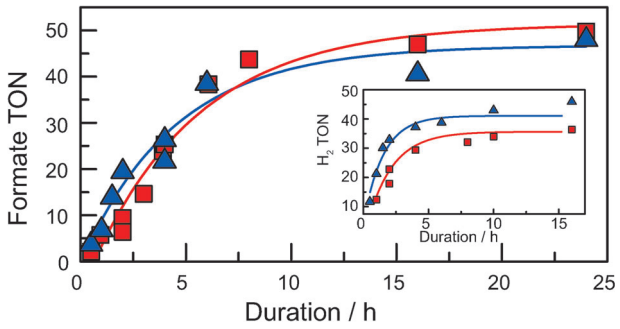

Figure 2. Equivalents of formate produced as a function of time for the photolyses of 1.4 mg of 10%-Cp*Rh@UiO-67 (■) and 0.1 mM of (**2**) (▲) under standard conditions described within the main text. Production of H_2 is presented within the inset.

early time point TOFs for formate production by 10%-Cp*Rh@UiO-67 and **2** are found to be 7.5 hr^{-1} and 10 hr^{-1} respectively (Supporting Information, Table S4). This situation is different for H_2 production (Figure 2, inset) as **2** is found to produce H_2 (TOF = 14 hr^{-1}) more efficiently than 10%-

Cp*Rh@UiO-67 (TOF = 5.4 hr^{-1}) (SI, Table S4). Therefore, by disfavoring the generation of H_2, 10%-Cp*Rh@UiO-67 can achieve nearly a two-fold increase in initial kinetic selectivity for formate over H_2. The overall stability was also comparable for both systems and the loss of activity during the photolysis has been attributed to the decomposition of the $[Ru(bpy)_3]Cl_2$ photosensitizer over several hours. This was determined by NMR experiments and via the recovery of activity upon the addition of more $[Ru(bpy)_3]Cl_2$ solution after 6 h of photolysis (Supporting Information, pp. S12 and S13).

Given the comparable activity observed between the heterogeneous and homogeneous systems, careful attention was focused on determining if the Rh complex is retained within the MOF host structure during catalysis or whether it is leached out. First, ^1H NMR analysis of the reaction mixtures after photolysis assays did not reveal any evidence of Cp*Rh being liberated from the MOF. Second, recyclability of a 10%-Cp*Rh@UiO-67 sample was demonstrated (Supporting Information, Figure S10). The facile nature in which heterogeneous catalysts can be re-isolated and re-used while maintaining intrinsic activity represents a major benefit over analogous homogeneous systems. The same 4 mg sample of 10%-Cp*Rh@UiO-67 could be recycled up to 6 times (16 h photolysis each run) with approximately 90% of the material re-isolated after each run. The 10% loss is primarily attributed to the small sample size being continually handled and is more representative of quite low total catalysts loss from the perspective of mass lost. Overall, 80% catalytic activity towards formate production was retained even after 4 days of cumulative photolysis time. The retention of the activity of the sample indicates that the active rhodium-based catalyst is retained within the heterogeneous framework. Furthermore, the parentage of formate was confirmed to be CO_2 as utilization of $^{13}CO_2$ resulted in a strongly enhanced ^{13}C NMR resonance corresponding to formate at $\delta =$ 169 ppm (Supporting Information, Figure S14). The latter observations corroborate the fact that assays performed in the absence of CO_2 do not yield any detectable carbon-containing reduction products, providing a robust confirming that CO_2 is the primary source for formate production.

Figure 3 shows the effect of increasing the amount of rhodium in Cp*Rh@UiO-67 on the initial rates of formate and H_2 production. For comparison the effect of increasing the concentration of **2** in the homogeneous system is also shown in Figure 3.

Under homogeneous conditions, increasing the concentration of **2** above 0.1 mM (Figure 3b) led to a drastic inactivation of the system, with almost no production of either formate or H_2 at 0.6 mM of **2**. In contrast, the heterogeneous system was much more stable with the rate of total product formation reaching a plateau above a 10% Rh incorporation into the UiO-67 framework. While Figure 3a shows that between 5%- and 10%-Rh incorporation the rates of formate and H_2 production nearly doubles, beyond 10% Rh incorporation the H_2/formate ratio increased as a function of increasing amounts of rhodium incorporation, with the formate production decreasing by approximately the same amount as the H_2 production increased. These data indicate that 10%-Cp*Rh@UiO-67 repre-

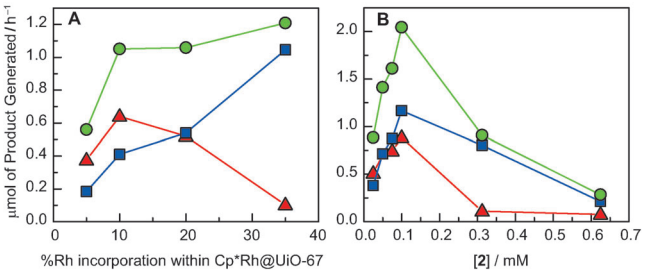

Figure 3. Effect of rhodium catalyst loading on the rate of μmols of formate produced (▲), H_2 production produced (■), and total products generated (●) per hour for the heterogeneous Cp*Rh@UiO-67 (a) and homogeneous solution of **2** (b). a) Different rhodium catalyst loadings were obtained by varying the %Rh molar incorporation within Cp*Rh@UiO-67. All samples contained 1.4 mg of MOF sample in 0.8 mL of the reaction mixture and results are reported as the quantities detected for each sample. b) Rhodium catalyst loadings were altered by varying the concentration of **2** in the 0.8 mL of the reaction solution. Quantities of products detected are reported based on values found per each sample.

sents a near-optimal %Rh incorporation for formate production and that the ratio of formate to H_2 produced can be tuned based on %Rh incorporation. Additionally, it confirms that Cp*Rh catalyst at or below 10% molar incorporation occupy active sites that have formate productivity comparable to that of the homogeneous photocatalytic system (e.g. 0.64 vs. 0.88 μmol hr^{-1} for the solid with 10%-Rh incorporation vs. the complex **2** at 0.1 mM concentration). The observation of decreased activity of **2** at higher concentrations in solution but constant activity of **2** at high loadings when immobilized within UiO-67 suggests that the MOF might additionally provide a catalyst stabilization by disfavoring possibly bimetallic deactivation pathways via site isolation of catalytic centers.

It is remarkable that the overall activity remains constant upon increasing Cp*Rh-catalyst loadings above 10% (Figure 3a) suggesting that the increased formation of H_2 and the decreased formation of formate are likely coupled. This can be assigned to the catalytic activity of Cp*Rh@UiO-67 towards formate dehydrogenation, leading to CO_2 and H_2, which has precedent for similar homogeneous compounds.[25] To observe this reactivity specifically with the Cp*Rh@UiO-67 system, 2 mg of 35%- Cp*Rh@UiO-67 were added to 1 mL of a CO_2 saturated ACN:TEOA (5:1, *v*:*v*) solution containing 22.1 mM sodium formate. The mixture was maintained at room temperature and shielded from direct light for 18 hrs during which time the formate concentration was found to decrease to 13.3 mM (Supporting Information, Figure S11). This corresponds to an approximate rate of formate decomposition of 0.25 μmol hr^{-1} mg^{-1} for 35%-Cp*Rh@UiO-67 under these conditions. This is the first report of a MOF catalyzing thermal decomposition of formate into H_2. It is likely that 10% Rh incorporation in Cp*Rh@UiO-67 generates the optimal balance between CO_2 reduction to formate and formate decomposition to H_2 for maximal formate production. Below 10%, there is likely good accessibility of the external photosensitizer to the catalytic sites, favouring CO_2 reduction by the Rh centers. Above 10%, in agreement with the decreased porosity beyond that limit (Figure 1a) inhibiting the access of the photosensitiz-

er, thermal decomposition of formate by the rhodium centers is favoured.

In summary, we have demonstrated for the first time the ability to photosensitize a molecular rhodium-based catalytic system and found conditions for an efficient reduction of CO_2 into formate. Furthermore, we have shown that it is possible, using post-synthetic exchange approaches, to heterogenize such complexes in the form of a rhodium-functionalized metal–organic framework (MOF), with the possibility to synthetically control the amount of active species grafted in the cavities. This new material allowed us to set up the first photocatalytic system for CO_2 reduction using a catalytic MOF and an homogeneous photosensitizer. Remarkably, the MOF catalyst, at low rhodium loadings, retains the activity of the homogeneous system but displays higher initial rate selectivity for formate and unprecedented stability and recyclability. In contrast, larger loading results in a loss of formate selectivity which we show is due to formate decomposition into CO_2 and H_2 catalyzed by the functionalized MOF itself. This demonstrates that, beyond single site isolation, special attention should be paid to find the optimum site density in the design of hybrid solid catalysts in order to avoid undesired side-reactions. We strongly believe that this account will stimulate the development of new functionalized MOFs thus offering a possible versatile and efficient platform for selective CO_2 photoreduction catalysis.

Experimental Section

Experimental and computational details are reported in the Supporting Information.

Acknowledgements

We acknowledge support from the Fondation de l'Orangerie for individual philanthropy and its donors, the French National Research Agency (Carbiored ANR-12-BS07-0024-03), the French State Program "Investissements d'Avenir" (Grant "LABEX DYNAMO", ANR-11-LABEX-0011) and the CNRS-Cellule Energie. The authors would like to thank Lise Marie Chamoreau for assistance in the data collection fort the crystal structure of complex ***2****. N.E. acknowledges the Direction Générale de l'Armement (DGA) for a graduate research fellowship.*

Keywords: carbon dioxide reduction · hydrogen · metal–organic frameworks · photocatalysis · rhodium

[1] For selected recent Reviews, see: a) E. E. Benson, C. P. Kubiak, A. J. Sathrum, J. M. Smieja, *Chem. Soc. Rev.* **2009**, *38*, 89 – 99; b) H. Arakawa, M. Aresta, J. N. Armor, M. A. Barteau, E. J. Beckman, A. T. Bell, J. E. Bercaw, C. Creutz, E. Dinjus, D. A. Dixan, K. Domen, D. L. DuBois, J. Eckert, E. Fujita, D. H. Gibson, W. A. Goddard, D. W. Goodman, J. Keller, G. J. Kubas, H. H. Kung, J. E. Lyons, L. E. Manzer, T. J. Marks, K. Morokuma, K. M. Nicholas, R. Periana, L. Que, J. Rostrup-Nielson, W. M. H. Sachtler, L. D. Schmidt, A. Sen, G. A. Somorjai, P. C. Stair, B. R. Stults, W. Tumas, *Chem. Rev.* **2001**, *101*, 953 – 996; c) J. L. Inglis, B. J. Maclean, M. T. Pryce, J. G. Vos, *Coord. Chem. Rev.* **2012**, *256*, 2571 – 2600; d) C. Costentin, M. Robert, J.-M. Saveant, *Chem. Soc. Rev.* **2013**, *42*, 2423 – 2436; e) J. Qiao, Y. Liu, F. Hong, J. Zhang, *Chem. Soc. Rev.* **2014**, *43*, 631 – 675; f) A. J. Morris, G. J. Meyer, E. Fujita, *Acc. Chem. Res.* **2009**, *42*, 1983 – 1994; g) H. Takeda, O. Ishitani, *Coord. Chem. Rev.* **2010**, *254*, 346 – 354; h) Y. Izumi, *Coord. Chem. Rev.* **2013**, *257*, 171 – 186; i) C. D. Windle, R. N. Perutz, *Coord. Chem. Rev.* **2012**, *256*, 2562 – 2570.

[2] a) D. J. Cole-Hamilton, *Science* **2003**, *299*, 1702 – 1706; b) L.-N. He, J.-Q. Wang, J.-L. Wang, *Pure Appl. Chem.* **2009**, *81*, 2069 – 2080; c) M. P. Conley, C. Coperet, *Top. Catal.* **2014**, *57*, 843 – 851.

[3] For selected recent Reviews, see: a) J. Mao, K. Li, T. Peng, *Catal. Sci. Technol.* **2013**, *3*, 2481 – 2498; b) S. C. Roy, O. K. Varghese, M. Paulose, C. A. Grimes, *ACS Nano* **2010**, *4*, 1259 – 1278; c) M. Gattrell, N. Gupta, A. Co, *J. Electroanal. Chem.* **2006**, *594*, 1 – 19; d) D. T. Whipple, P. J. A. Kenis, *J. Phys. Chem. Lett.* **2010**, *1*, 3451 – 3458; e) D. Uner, M. M. Oymak, *Catal. Today* **2012**, *181*, 82 – 88; f) S. Navalón, A. Dhakshinamoorthy, M. Álvaro, H. Garcia, *ChemSusChem* **2013**, *6*, 562 – 577.

[4] a) X. S. Zhao, X. Y. Bao, W. Guo, F. Y. Lee, *Mater. Today* **2006**, *9*, 32 – 39; b) U. Diaz, M. Boronat, A. Corma, *Proc. R. Soc. London Ser. A* **2012**, *468*, 1927 – 1954; c) Q. Chen, *Curr. Org. Chem.* **2013**, *17*, 1303 – 1324; d) Q. Chen, *Curr. Org. Chem.* **2013**, *17*, 1303 – 1324.

[5] a) M. J. Ingleson, J. P. Barrio, J. B. Guilbuad, Y. Z. Khimyak, M. J. Rosseinsky, *Chem. Commun.* **2008**, 2680 – 2682; b) C. J. Doonan, W. Morris, H. Furukawa, O. M. Yaghi, *J. Am. Chem. Soc.* **2009**, *131*, 9492 – 9493; c) K. K. Tanabe, S. M. Cohen, *Angew. Chem. Int. Ed.* **2009**, *48*, 7424 – 7427; *Angew. Chem.* **2009**, *121*, 7560 – 7563; d) X. Zhang, F. Llabres, A. Corma, *J. Catal.* **2009**, *265*, 155 – 160; e) E. D. Bloch, D. Britt, C. Lee, C. J. Doonan, F. J. Uribe-Romo, H. Furukawa, J. R. Long, O. M. Yaghi, *J. Am. Chem. Soc.* **2010**, *132*, 14382 – 14384; f) S. Chavan, J. G. Vitillo, M. J. Uddin, F. Bonino, C. Lamberti, E. Groppo, K.-P. Lillerud, S. Bordiga, *Chem. Mater.* **2010**, *22*, 4602 – 4611; g) S. Bhattacharjee, D.-A. Yang, W.-S. Ahn, *Chem. Commun.* **2011**, *47*, 3637 – 3639; h) J. Canivet, S. Aguado, Y. Schuurman, D. Farruseng, *J. Am. Chem. Soc.* **2013**, *135*, 4195 – 4198; i) S. Pullen, H. Frei, A. Orthaber, S. M. Cohen, S. Ott, *J. Am. Chem. Soc.* **2013**, *135*, 16997 – 17003.

[6] a) T. Zhang, F. Song, W. Lin, *Chem. Commun.* **2012**, *48*, 8766 – 8768; b) B. Pugin, *J. Mol. Catal. A* **1996**, *107*, 273 – 279.

[7] a) D. Esken, X. Zhang, O. I. Lebedev, F. Schroder, R. A. Fischer, *J. Mater. Chem.* **2009**, *19*, 1314 – 1319; b) Y. B. Huang, Z. J. Lin, R. Cao, *Chem. Eur. J.* **2011**, *17*, 12706 – 12712; c) M. Meilikhov, K. Yusenko, D. Esken, S. Turner, G. Van Tendeloo, R. A. Fischer, *Eur. J. Inorg. Chem.* **2010**, 3701 – 3714; d) M. Müller, S. Turner, O. I. Lebedev, Y. M. Wang, G. van Tendeloo, R. A. Fischer, *Eur. J. Inorg. Chem.* **2011**, 1876 – 1887.

[8] a) C. C. Guo, J. X. Song, X. B. Chen, G. F. Jiang, *J. Mol. Catal. A* **2000**, *157*, 31 – 40; b) H. U. Blaser, B. Pugin, F. Spindler, A. Togni, *C. R. Chim.* **2002**, *5*, 379 – 385; c) A. Dervisi, C. Carcedo, L. Ooi, *Adv. Synth. Catal.* **2006**, *348*, 175 – 183; d) M. H. Alkordi, Y. Liu, R. W. Larsen, J. F. Eubank, M. Eddaoudi, *J. Am. Chem. Soc.* **2008**, *130*, 12639 – 12641.

[9] a) C. Copéret, M. Chabanas, R. P. Saint-Arroman, J. M. Basset, *Angew. Chem. Int. Ed.* **2003**, *42*, 156 – 181; *Angew. Chem.* **2003**, *115*, 164 – 191; b) C. E. Song, D. H. Kim, D. S. Choi, *Eur. J. Inorg. Chem.* **2006**, 2927 – 2935; c) J. M. Thomas, R. Raja, *Acc. Chem. Res.* **2008**, *41*, 708 – 720; d) V. Dal Santo, F. Liguori, C. Pirovano, M. Guidotti, *Molecules* **2010**, *15*, 3829 – 3856; e) J. M. Thomas, *Phys. Chem. Chem. Phys.* **2014**, *16*, 7647 – 7661.

[10] H. Fei, J. Shin, Y. S. Meng, M. Adelhardt, J. Sutter, K. Meyer, S. M. Cohen, *J. Am. Chem. Soc.* **2014**, *136*, 4965 – 4973.

[11] a) C. Wang, Z. Xie, K. E. deKrafft, W. Lin, *J. Am. Chem. Soc.* **2011**, *133*, 13445 – 13454; b) J. Lou, L. Li, S. Zhang, L. Xu, J.-Y. Wang, L.-X. Shi, Z.-N. Chen, M. Hong, *Chem. Sci.* **2014**, *5*, 3808 – 3813.

[12] C. H. Hendon, D. Tiana, M. Fontecave, C. Sanchez, L. D'arras, C. Sassoye, L. Rozes, C. Mellot-Draznieks, A. Walsh, *J. Am. Chem. Soc.* **2013**, *135*, 10942 – 10945.

[13] E. Steckhan, S. Hermann, R. Ruppert, E. Dietz, M. Frede, E. Spika, *Organometallics* **1991**, *10*, 1568 – 1577.

[14] C. Caix, S. Chardon-Noblat, A. Deronzier, *J. Electroanal. Chem.* **1997**, *434*, 163 – 170.

[15] a) Q. Liu, L. Wu, S. Gulak, N. Rockstroh, R. Jackstell, M. Beller, *Angew. Chem. Int. Ed.* **2014**, *53*, 7085 – 7088; *Angew. Chem.* **2014**, *126*, 7205 – 7208; b) A. Boddien, F. Gartner, C. Federsel, P. Sponholz, D. Mellmann, R. Jackstell, H. Junge, M. Beller, *Angew. Chem. Int. Ed.* **2011**, *50*, 6411 – 6414; *Angew. Chem.* **2011**, *123*, 6535 – 6538; c) A. Boddien, B. Loges, H. Junge, M. Beller, *ChemSusChem* **2008**, *1*, 751 – 758; d) S. Zhang, P. Kang,

S. Ubnoske, M. K. Brennaman, N. Song, R. L. House, J. T. Glass, T. J. Meyer, *J. Am. Chem. Soc.* **2014**, *136*, 7845 – 7848; e) P. Kang, S. Zhang, T. J. Meyer, M. Brookhart, *Angew. Chem. Int. Ed.* **2014**, *53*, 8709 – 8713; *Angew. Chem.* **2014**, *126*, 8853 – 8857.

[16] a) D. Mellman, E. Barsch, M. Bauer, K. Grabow, A. Boddien, A. Kammer, P. Sponholz, U. Bentrup, R. Jackstell, H. Junge, G. Laurenczy, R. Ludwig, M. Beller, *Chem. Eur. J.* **2014**, *20*, 13589 – 13602; b) J. Joo, T. Uchida, A. Cuesta, M. T. Koper, M. Osawa, *Electrochim. Acta* **2014**, *129*, 127 – 136; c) H. Wang, L. Aldoen, F. J. DiSalovo, H. D. Abruna, *Phys. Chem. Chem. Phys.* **2008**, *10*, 3739 – 3751.

[17] a) U. Kölle, M. Grützel, *Angew. Chem. Int. Ed. Engl.* **1987**, *26*, 567 – 570; *Angew. Chem.* **1987**, *99*, 572 – 574; b) E. Kumaran, W. K. Leong, *Organometallics* **2012**, *31*, 1068 – 1072.

[18] J. H. Cavka, S. Jakobsen, U. Olsbye, N. Guillou, C. Lamberti, S. Bordiga, K. P. Lillerud, *J. Am. Chem. Soc.* **2008**, *130*, 13850 – 13851.

[19] S. Chavan, J. G. Vitillo, D. Gianolio, O. Zavorotynska, B. Civalleri, S. Jakobsen, M. H. Nilsen, L. Valenzano, C. Lamberti, K. P. Lillerud, S. Bordiga, *Phys. Chem. Chem. Phys.* **2012**, *14*, 1614 – 1626.

[20] a) W. A. Maza, A. J. Morris, *J. Phys. Chem. C* **2014**, *118*, 8803 – 8817; b) W. A. Maza, S. R. Ahrenholtz, C. C. Epley, C. S. Day, A. J. Morris, *J. Phys. Chem. C* **2014**, *118*, 14200 – 14210.

[21] K. T. Butler, C. H. Hendon, A. Walsh, *J. Am. Chem. Soc.* **2014**, *136*, 2703 – 2706.

[22] T. Yui, Y. Tamaki, K. Sekizawa, O. Ishitani, *Top. Curr. Chem.* **2011**, *303*, 151 – 184.

[23] H. Takeda, H. Koizumi, K. Okamoto, O. Ishitani, *Chem. Commun.* **2014**, *50*, 1491 – 1493.

[24] a) M. L. Clark, K. A. Grice, C. E. Moore, A. L. Rheingold, C. P. Kubiak, *Chem. Sci.* **2014**, *5*, 1894 – 1900; b) J. M. Smieja, C. P. Kubiak, *Inorg. Chem.* **2010**, *49*, 9283 – 9289.

[25] a) Y. Himeda, S. Miyazawa, T. Hirose, *ChemSusChem* **2011**, *4*, 487 – 493; b) C. Creutz, M. H. Chou, *J. Am. Chem. Soc.* **2009**, *131*, 2794 – 2795; c) Y. Himeda, N. Onozawa-Komatsuzaki, H. Sugihara, H. Arakawa, K. Kasuga, *Organometallics* **2004**, *23*, 1480 – 1483.

Received: December 4, 2014
Published online on January 22, 2015